chemosensors

MDPI

Supplementary materials

Selective Outdoor Humidity Monitoring Using Epoxybutane Polyethyleneimine in a Flexible Microwave Sensor

Bernard Bobby Ngoune [1,*], Hamida Hallil [1,*], Bérengère Lebental [2], Guillaume Perrin [2], Shekhar Shinde [3], Eric Cloutet [3], Julien George [4], Stéphane Bila [4], Dominique Baillargeat [4] and Corinne Dejous [1]

[1] University of Bordeaux, CNRS, Bordeaux INP, IMS, UMR 5218, F-33400 Talence, France
[2] COSYS-IMSE, Université Gustave Eiffel, F-77420 Marne-La-Vallée, France
[3] University of Bordeaux, CNRS, Bordeaux INP, LCPO, UMR 5629, F-33600 Pessac, France
[4] University of Limoges, CNRS, XLIM UMR 7252, F-87060 Limoges, France
* Correspondence: bernard-bobby.ngoune@u-bordeaux.fr (B.B.N.); hamida.hallil-abbas@u-bordeaux.fr (H.H.)

1. Sensor Design, Fabrication and Characterisation

Figure S1a illustrates the flexed fabricated sensor. The thickness of the deposited sensitive material is measured using a numerical microscope KEYENCE VHX-500. Due to the transparent nature of the polymer a few nanometres of platinum are sputtered on the control sample before thickness measurement. Figure S1b and Figure S1c show the water contact angle measurement of the Kapton substrate and of the EB-PEI, respectively, 34.8 ± 10.5° and 28.2 ± 5.3°., measured using a contact angle goniometer (Kruss Germany).

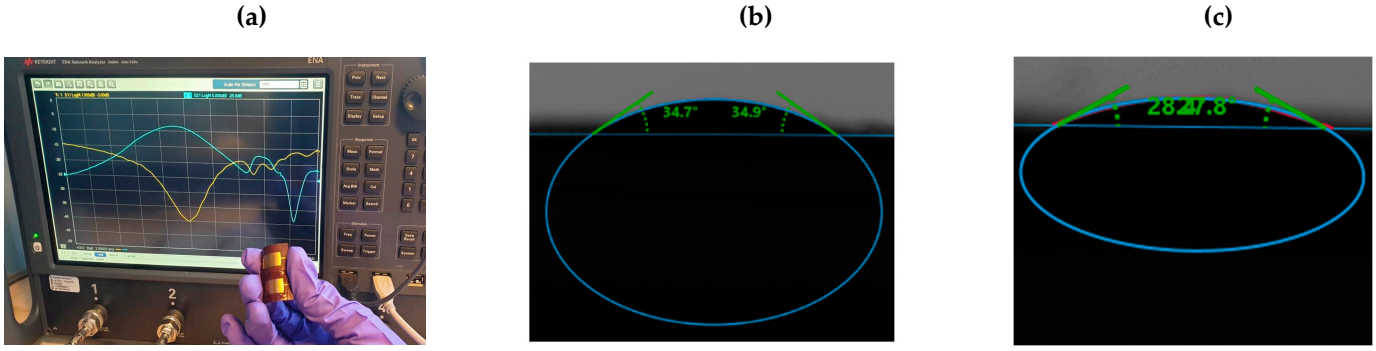

Figure S1. (**a**) The flexed fabricated sensor with EB-PEI-coated and bare resonators and typical scattering parameters characterisation with Vector Network Analyzer. (**b**) Water contact angle measurement on the Kapton substrate. (**c**) Water contact angle measurement of EB-PEI.

2. Parameter Extraction from Sensor Response

The variation of the sensor's electrical properties such as permittivity and conductivity are measured as a change in the magnitude and phase of the S parameters, as shown in Figure S2 [1]. The sensing response is extracted for both the bare and the coated resonators in order to obtain a differential measurement. The raw spectra obtained from the vector network analyser (VNA) are first filtered using time gating (centre = 0 ns and span = 200 ns) in order to remove any potential spurious electromagnetic signals, thus reducing the noise.

We extract Δfrequency (change in resonance frequency) and Δmagnitude (change in magnitude at resonance frequency) of the coated (sen) and bare (ref) resonator S parameters, as well as the difference between them. Resonance corresponds to the minimum of the S_{11} magnitude spectrum, as in Figure S2a. A 1 dB confidence window is used to locate the curve minimum in order to reduce the noise due to the limited number of frequency points: we first locate point A, corresponding to the minimum obtained directly, then we increment the magnitude at A by 1 dB to obtain points B and C with enhanced accuracy thanks to a greater curve slope and corresponding to the confidence window. The

resulting resonance frequency is the average of frequencies at points B and C, as shown in equation 1. The resulting magnitude at resonance is determined by interpolation.

$$F_{res} = (f_B + f_C)/2 \quad (1)$$

Δphase (change in phase at constant frequency) and Δphasefrequency (change in frequency at a constant phase) are extracted from the S_{11} phase spectrum obtained from the network analyser, as shown in Figure S2b.

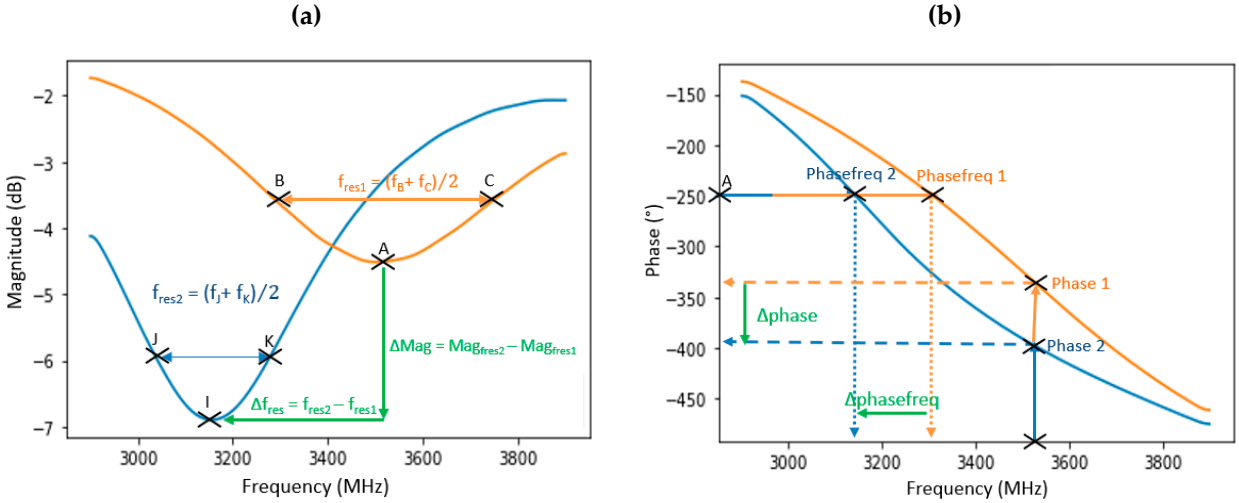

Figure S2. Response extraction from (**a**) S_{11} magnitude spectrum (**b**) S_{11} phase spectrum.

3. Experimental Setups

Two test benches are used to characterise the sensors for RH, temperature and gases in laboratory conditions, as shown in Figure S3. Figure S3a shows a test bench for sensor characterisation under different vapours and low RH (0 – 30%). It consists of a calibration gas generator (PUL110), a four-port VNA, a home-designed RF sensor test cell and a commercial temperature and humidity sensor (SHT85) placed along the gas flow, an Arduino and a PC. The vapor generator works by heating a liquid in a permeation tube, thereby creating a vapour phase, which is diluted by the mass flow controllers to obtain different vapour concentrations in a carrier gas, dry air or nitrogen, at constant flow. The setup is placed in an air-conditioned room at a temperature of 20°C. Figure S3b shows a climatic chamber used to generate RH in air (30–90%) at different temperatures. A ramp function is used whilst changing the RH setpoint in order to avoid spurious vibrations of the climatic chamber. The RF sensor and the commercial temperature and humidity sensor are placed in the same test cells with gas inlet and outlet, as in Figure S3a.

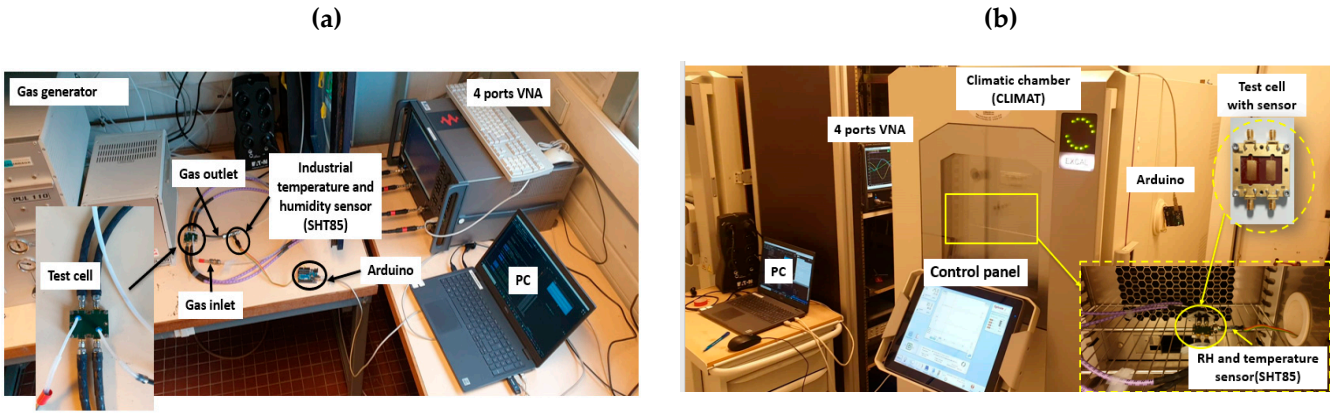

Figure S3. A two-port portable Anritsu VNA was used for S parameter acquisition, Raspberry Pi 4 was used to control the VNA and two 50 ohms caps were used as loads at the open outputs of the test cell. Gas analysers from Envea were used to provide reference measurements of NO, NO_2, O_3, CO and CO_2 gases.

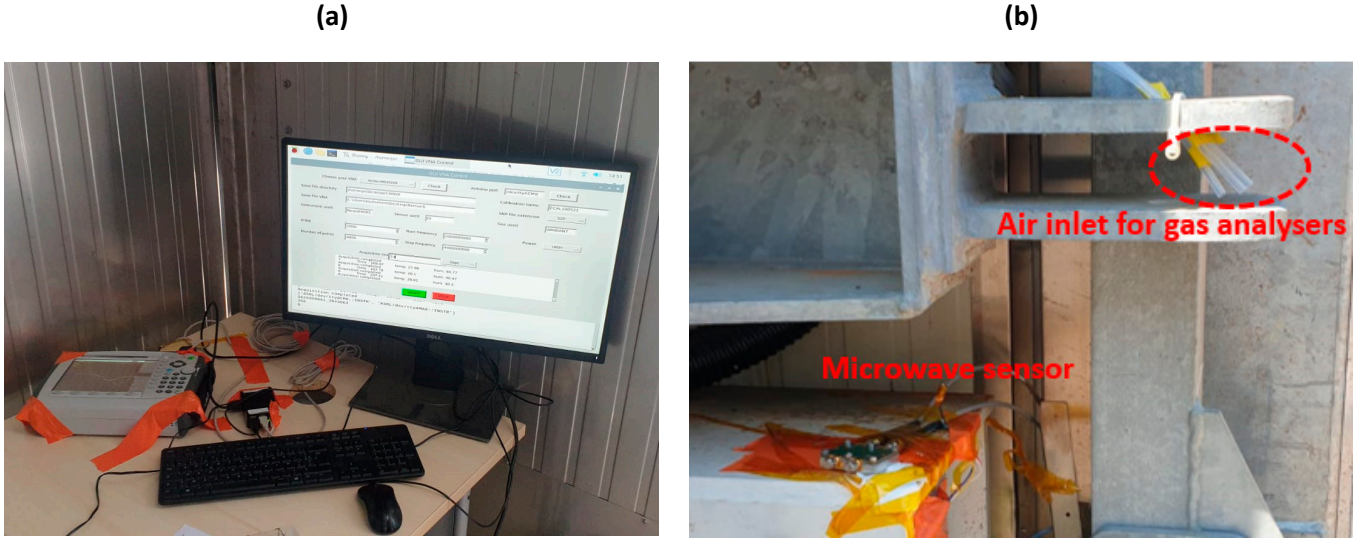

Figure S4. Outdoor experimental sensing setup: (**a**) instrumentation placed indoor, (**b**) sensor placed outdoor with air inlet for the gas analysers from Envea: AC32e for NO and NO_2, O342e for O_3 and CO12e for CO and CO_2.

4. Magnitude Response to Humidity and Temperature in Lab Conditions

Figures S5a-c describe the dynamical S_{11} magnitude response characteristics when the sensor was exposed to humidity in the overall range of 0–90% RH (0–30% RH, 35–75% RH and 80–90% RH, respectively, at 20°C), and Figures S5d-e show, respectively, the sensor's magnitude response calibration curve and the resulting linear curve in Log response. The sensor exhibits the different sensitivities of -0.0033 dB/%RH, -0.0304 dB/%RH and -0.171 dB/%RH in the ranges of 0–30% RH, 35–75% RH and 80–90% RH, respectively, as shown by the fitted lines with their corresponding coefficient of determination (COD) in Figure S5d. The Figure S5f shows the superposition of sorption and desorption magnitude responses, highlighting the low hysteresis, less than 1%, in the range 35–75% RH.

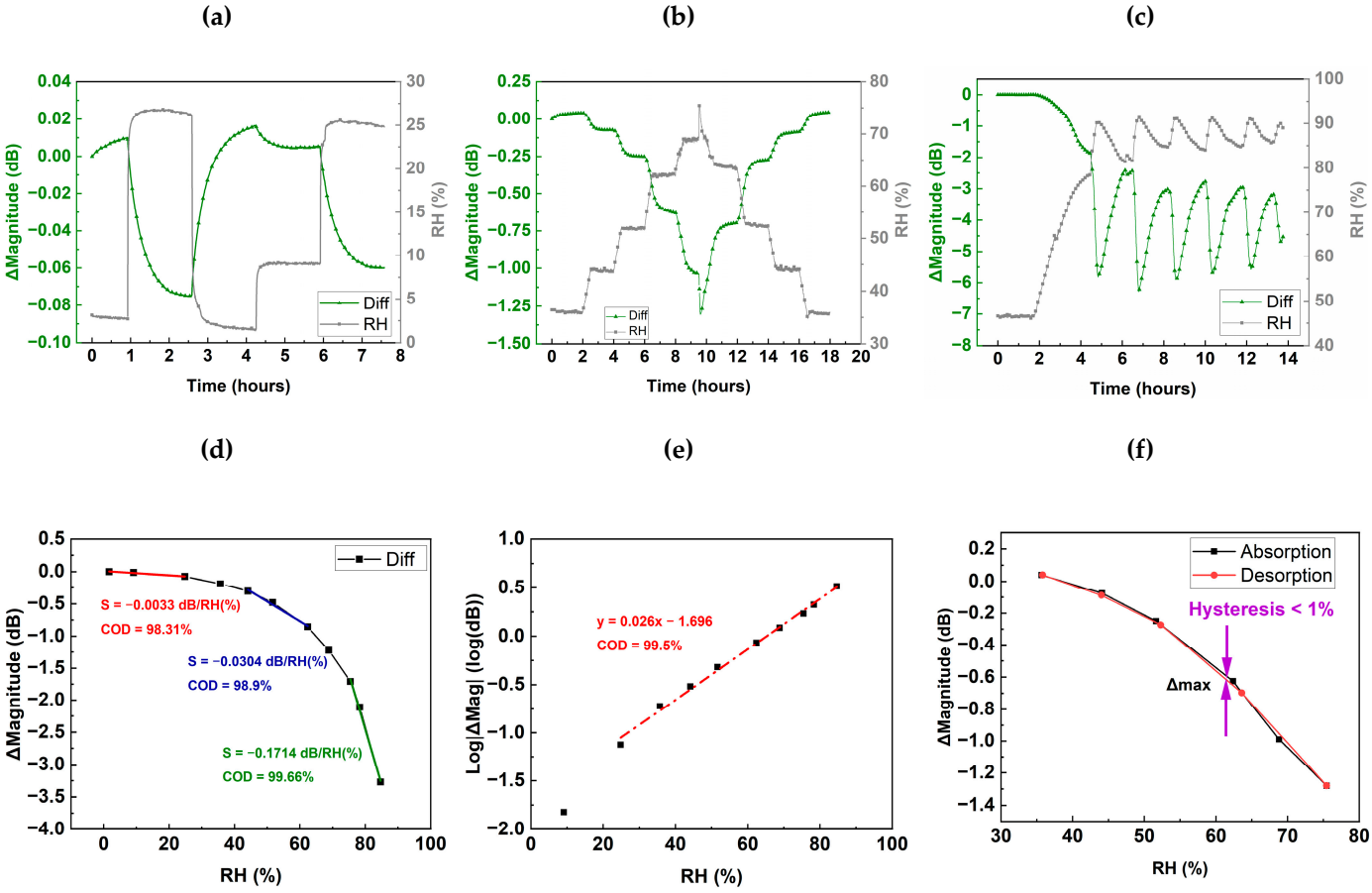

Figure S5. Sample 1 magnitude response to RH: dynamic magnitude response in the range 0%–30% RH (**a**), 35%–75% RH (**b**) and 80%–90% RH (**c**); (**d**) sensor RH calibration curve with its sensitivities and CODs per RH range, (**e**) sensor Log magnitude response and (**f**) superposition of sorption and desorption responses and hysteresis in the range 35–75% RH.

Figure S6a–b shows the sensor's magnitude response desorption and absorption drift when exposed to dry N_2 gas and constant 45% RH, respectively. In both cases, the curves show the results after at least twice the response time (90 minutes) exposure, where surface interaction mechanisms of the coated resonator are supposed to be already in steady state, thus nonvisible, so that bulk interaction mechanisms become visible, if any, as well as possible drifts due to other phenomena. As for the frequency, the differential response in magnitude enables to compensate for drifts, though a very small differential signal remains. The sensor shows linear curves in Figure S6a, with a 0.0145 dB/hour slope for the coated resonator and 0.018 dB/hour for the bare resonator when exposed to N_2 gas with a drying effect. This results in a differential response for long-term desorption of -0.003 dB/hour (which could induce an error in ambient humidity variation estimation of ~0.91 %RH/hour). On the other hand, a linear sorption drift of -0.002 dB/hour (~0.67 %RH/hour) when exposed to constant 45% RH is observed in Figure S6b, resulting from -0.0017 dB/hour for the coated resonator and -0.004 dB/hour for the bare resonator.

The response and recovery time extracted from a typical magnitude response RH at 20 °C is shown in Figure S6c (45/45 minutes, respectively). Not surprisingly, the magnitude response/recovery times are very similar to those obtained from the frequency response.

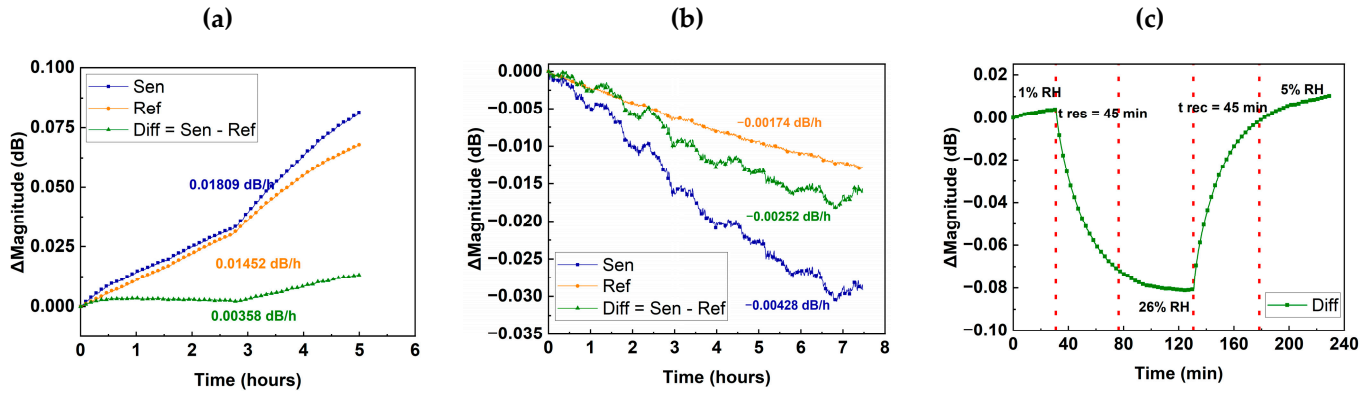

Figure S6. Magnitude response (**a**) sensor desorption drift when exposed to $\mathbf{N_2}$ gas at 20°C (**b**), sensor absorption drift and stability when exposed to constant 45% RH and (**c**) response and recovery times at 20 °C extracted from the magnitude response

The Figure S7 reports the sensor differential behaviour with temperature. A linear temperature sensitivity of -0.0178 dB/°C was recorded, as shown on the calibration curve in Figure S7b. Temperature causes a variation in the IDTs impedance and in the electrical properties of the sensitive material, resulting in a shift in magnitude, similarly as in resonance frequency.

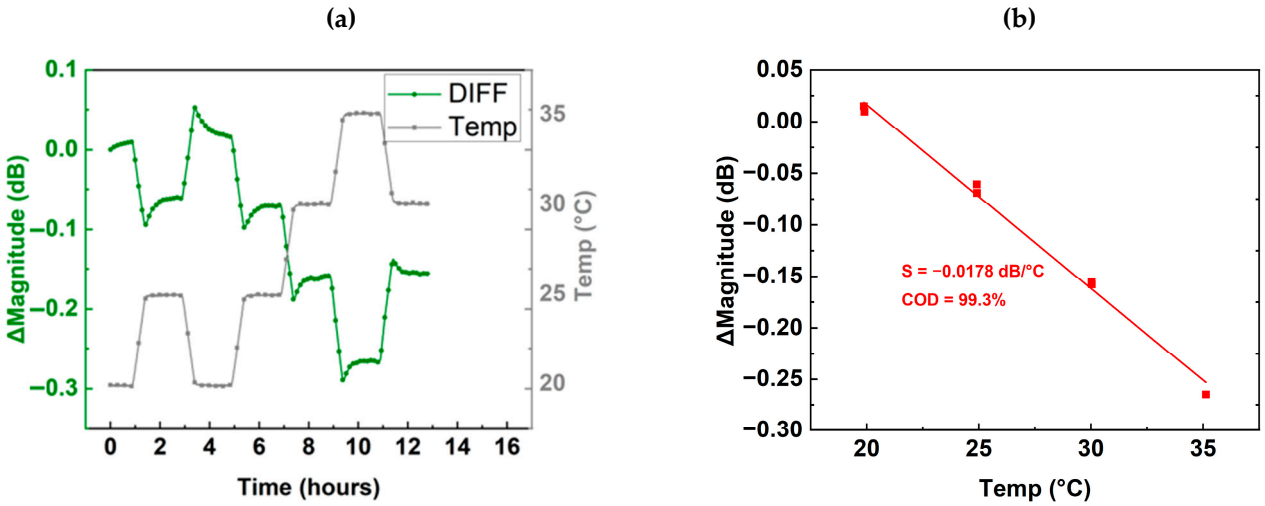

Figure S7. (**a**) Temperature dynamic frequency response in the range 20–35°C and (**b**) sensor temperature calibration curve with its sensitivity and COD.

5. Variance-Based Sensitivity Analysis in Environmental Conditions

The microwave sensor was exposed to real environmental conditions between August 26th and September 2nd 2021 in the Sense-City platform. Four responses, FreqDif (MHz), PhasefreqDif (MHz), MagnDif (dB) and PhaseDif (°), are considered as outputs. Six environmental parameters (RH, temperature, NO, NO_2, O_3, CO and CO_2 gases) measured by the Vaisala weather station and the Envea gas analysers are considered as inputs. When focusing on relations between sensor outputs and inputs, the sensor outputs seem to be affected by RH and temp but also by O_3, NO_x and CO_2. To be more precise in these analyses, a variance decomposition of the output signals was carried out, the results are shown in Figure S8. The main effects characterise the influence of each input on its own (no interaction with other inputs); the total effects quantify the total influence of each input, including interactions with other inputs. RH and temperature are the two main factors influencing the sensor outputs (higher main and total effects), and among these two,

RH seems to be the dominant factor. A small sensitivity to O_3 and CO_2 is also observed (nonzero values for the total effects); above all, we can see an important role of input cross-effects on the output variability (the total effects are most of the time much higher than the main effects).

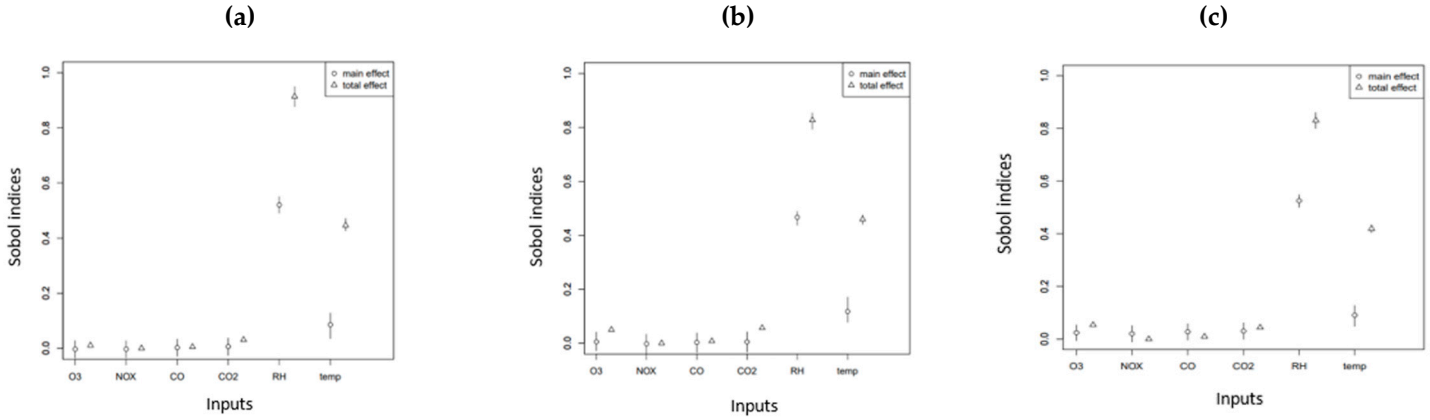

Figure S8. Sobol indices associated with the variance decomposition of the sensor outputs: (**a**) Freq, (**b**) Phasefreq and (**c**) Phase. The main effects characterise the influence of each input on its own (no interaction with other inputs); the total effects quantify the total influence of each input, including interactions with other inputs.

References

[1] Bahoumina, P.; Hallil, H.; Lachaud, J.L.; Abdelghani, A.; Frigui, K.; Bila, S.; Baillargeat, D.; Ravichandran, A.; Coquet, P.; Paragua, C.; et al. Microwave flexible gas sensor based on polymer multi wall carbon nanotubes sensitive layer. *Sens. Actuators B: Chem.* **2017**, *249*, 708–714. https://doi.org/10.1016/j.snb.2017.04.127.